Biochimica et Biophysica Acta 1838 (2014) 831–841

Contents lists available at ScienceDirect

Biochimica et Biophysica Acta

journal homepage: www.elsevier.com/locate/bbamem

Mutual structural effect of bilirubin and model membranes by vibrational circular dichroism

Pavlína Novotná [a], Iryna Goncharova [a], Marie Urbanová [b,*]

[a] Department of Analytical Chemistry, Institute of Chemical Technology, Prague, Technická 5, 166 28 Prague 6, Czech Republic
[b] Department of Physics and Measurements, Institute of Chemical Technology, Prague, Technická 5, 166 28 Prague 6, Czech Republic

ARTICLE INFO

Article history:
Received 10 July 2013
Received in revised form 7 December 2013
Accepted 9 December 2013
Available online 16 December 2013

Keywords:
Vibrational circular dichroism
Liposome
Bilirubin–lipid interaction
Bilirubin–polypeptide interaction
Sphingomyelin
Membrane structure

ABSTRACT

In this study, vibrational circular dichroism (VCD) spectroscopy was employed for the first time to study the bilirubin (BR) interaction with model membranes and models for membrane proteins. An enantioselective interaction of BR with zwitterionic 1,2-dimyristoyl-*sn*-glycero-3-phosphocholine (DMPC) and sphingomyelin (SPM) liposomes was observed by VCD and electronic circular dichroism (ECD) complemented by absorption and fluorescence spectroscopy. The M-form of BR was preferentially recognized in the BR/DMPC system at concentration above 1×10^{-4} M, for lower concentrations the P-form of BR was recognized by the DMPC liposomes. The VCD spectra also showed that the SPM liposomes, which represent the main component of nerve cell membrane, were significantly more disturbed by the presence of BR than the DMPC liposomes—a stable association with a strong VCD signal was observed providing the explanations for the supposed BR neurotoxicity. The effect of time and pH on the BR/DMPC or SPM liposome systems was shown to be essential while the effect of temperature in the range of 15–70 °C was negligible demonstrating the surprisingly high temperature stability of BR when interacting with the studied membranes. The influence of a membrane protein was tested on a model consisting of poly-L-arginine (PLAG) bound in the *α-helical* form to the surface of 1,2-dimyristoyl-*sn*-glycero-3-phospho-(1′-rac-glycerol) liposomes and sodium dodecyl sulfate micelles. VCD and also ECD spectra showed that a variety of BR diastereoisomers interacted with PLAG in such systems. In a system of PLAG with micelles composed of sodium dodecyl sulfate, the M-form of bound BR was observed.

1. Introduction

Bilirubin (BR), the final product of the hem catabolism in the human body, is formed at a rate of about 300 mg per day and performs both positive and negative functions [1]. Although, this pigment has been known for more than a century, its exact effects are still being debated [1–3]. Most BR is promptly eliminated from the body [2,4]. However, in the pathologic state, BR may accumulate and at higher concentrations its negative effects may appear [1,4]. During the hyperbilirubinemia of newborns, the deposition of unconjugated BR in the central nervous system is the major factor causing bilirubin encephalopathy.

In this article, we have focused on BR and membranes, the system modeling BR attack on the cell membrane surface related to BR neurotoxicity. The interaction of BR with cell membranes may have several different mechanisms which result in the differences in cell function or in cell death [5]. It is thought [2,6,7] that these neurotoxic effects of BR are caused by its bond to the membrane which is enantioselective.

Although BR is a linear tetrapyrrolic pigment, its structure is not planar. It takes helical forms composed of two rigid planar dipyrrole units, which may have either a P- or M-sense of helicity with different dihedral angles between the dipyrrole units [8–14] (Scheme 1). As the racemization barrier between these two forms is low, a racemic mixture of BR in a homogeneous solution without chiral agents is formed. Nevertheless, it has been observed previously [6,15] by the method of electronic circular dichroism (ECD) that the P- or M-form of BR interacted preferentially with models of membrane surfaces. This interaction probably caused damage [7,16–21] to the membrane which may result in the cell apoptosis. The ECD observations showed [6,7,22] that the BR interaction with membranes is strongly influenced by the chemical composition of the membrane.

The liposomes composed mainly of a phospholipid bilayer probably do not significantly change their structure after an interaction with BR [23] and mainly fulfill the role of its transporter. However, the interaction of BR with sphingomyelin (SPM) and gangliosides, which are the main components of nerve cell membranes, differs from that with phospholipids [6,15–17].

Different spectral methods [6,7,16,22–32] have been already employed to study the interactions of BR with model membranes.

Abbreviations: BR, bilirubin; DLS, dynamic light scattering; DMPC, 1,2-dimyristoyl-*sn*-glycero-3-phosphocholine; DMPG, 1,2-dimyristoyl-*sn*-glycero-3-phospho-(1′-rac-glycerol); DPPG, 1,2-dipalmitoyl-*sn*-glycero-3-phospho-(1′-rac-glycerol); ECD, electronic circular dichroism; HSA, human serum albumin; IR, infrared; LUV, large unilamellar vesicle; PLAG, poly-L-arginine; SPM, sphingomyelin; SDS, sodium dodecyl sulfate; UV–vis, ultraviolet–visible; VCD, vibrational circular dichroism

* Corresponding author. Tel.: +420 220443036; fax: +420 220444334.
E-mail address: Marie.Urbanova@vscht.cz (M. Urbanová).

0005-2736/$ – see front matter © 2013 Elsevier B.V. All rights reserved.
http://dx.doi.org/10.1016/j.bbamem.2013.12.005

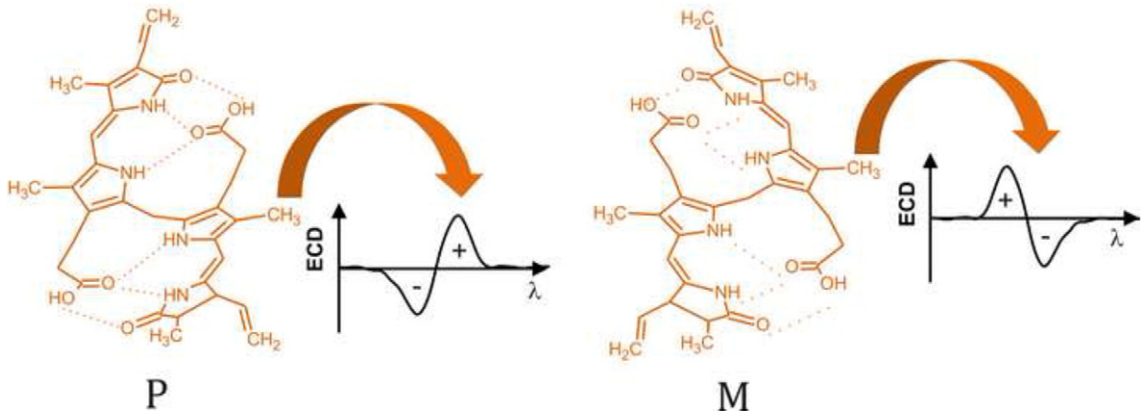

Scheme 1. Structure of the P- and M-helical form of BR in their global energy minimum with marked hydrogen bridges and the characteristic positive and negative ECD couplet for the P- and M-forms, respectively, observed in the region of BR absorption.

Most of these studies focus on the lipid part of the system. In this study, we employed mainly vibrational circular dichroism (VCD), a chiroptical method suitable for the simulation of locally high concentrations of BR, which are thought to be the main cause of its negative effects. Another advantageous aspect of this method is its local sensitivity to the chiral structures of BR [33–35] as well as model membranes [36]. In addition, ECD, the transmission absorption in the both IR (infrared) and UV–vis (Ultraviolet–visible) regions and fluorescence emission spectroscopy were employed.

The main aim of this article was to study the interactions of BR with model membranes and to show their mutual influence. We chose three different compositions of model membranes. Zwitterionic liposomes from 1,2-dimyristoyl-*sn*-glycero-3-phosphocholine (DMPC) were chosen to simulate the phospholipid bilayer and sphingomyelin (SPM) liposomes were used as a model for nerve cell membranes. The models used enabled the study of the influence of temperature and pH changes on these systems. Negatively charged liposomes composed of 1,2-dimyristoyl-*sn*-glycero-3-phospho-(1′-rac-glycerol) (DMPG) or 1,2-dipalmitoyl-*sn*-glycero-3-phospho-(1′-rac-glycerol) (DPPG) and micelles composed of sodium dodecyl sulfate (SDS) were then used to investigate the interactions of BR with membranes in the presence of a positively charged polypeptide poly-L-arginine (PLAG), which interacts with the DMPG or DPPG liposomes and the SDS micelles in its *α-helical* form [36]. PLAG represents a suitable model for membrane protein as it enabled the study of the interaction of BR with two different secondary conformations of a polypeptide: the α-helix when PLAG was bound to the membrane and a *polyproline II*-like structure in the solution.

2. Material and methods

2.1. Materials

The lipids 1,2-dimyristoyl-*sn*-glycero-3-phosphocholine (DMPC), sphingomyelin (SPM) and 1,2-dipalmitoyl-*sn*-glycero-3-phospho-(1′-rac-glycerol) sodium salt (DPPG) were purchased from Avanti Polar Lipids (Alabaster, AL). Lipid 1,2-dimirystoyl-*sn*-glycero-3-phospho-(1′-rac-glycerol) sodium salt (DMPG) was purchased from (CordenPharma International, Germany). Bilirubin-IXa (BR) was purchased from Frontier Scientific (USA). The sodium dodecyl sulfate (SDS), human serum albumin (HSA) protein and the poly-L-arginine hydrochloride polypeptide (approximately 184 amino acid units, PLAG) were purchased from Sigma Aldrich. Deuterated water (99.9% D, Chemotrade, Czech Republic) was used for the VCD measurements. All of the chemicals were used without further purification. For the structure of the used polypeptide and lipids, see Fig. S1 in Supplementary material.

2.2. Preparation of large unilamellar vesicles

The liposomes were prepared using the standard procedures [37]. The appropriate amount of dried lipid was weighed and dissolved in chloroform or a chloroform/methanol (for DMPG and DPPG) mixture (2:1, v/v) and vortexed for 5 min. The sample was dried under low pressure to form a thin film on the vial wall, after which it was left under high vacuum for 6 h. The film was then hydrated via the addition of a 1×10^{-2} M phosphate buffer with an appropriate pH and vortexed extensively. The resulting multilamellar liposome suspension was then reduced to uniform large unilamellar vesicles (LUVs) by passing twenty-three times through a polycarbonate membrane with a mean pore diameter of 100 nm using a Mini-Extruder (Avanti Polar Lipids). After extrusion, the LUVs were allowed to equilibrate for at least 2 h before use. The final lipid concentration was calculated based on the weight of the dried lipid [38–42]. For the VCD measurements, a deuterated phosphate buffer was used. During the liposome preparation, the D-H exchange took place, which can be observed in the mid IR.

The dynamic light scattering (DLS) method confirmed the narrow size distribution of the LUVs with the maximum at (110 ± 2) nm.

2.3. Sample preparation

The sodium salt of BR was prepared to obtain a BR of higher solubility [33]. Powdered BR was dissolved in a 3:1 excess of a sodium hydroxide aqueous solution. A complete neutralization was achieved and the solution was centrifuged. The dissolved part was cooled to the temperature of liquid nitrogen and lyophilized in the dark. The powder obtained was stored at −20 °C for no longer than 24 h.

The spectral measurements were conducted in the solutions of a phosphate buffer (deuterated for VCD). BR was dissolved in the 1×10^{-2} M phosphate buffer and its stock solution was then slowly added to the solution of the liposomes or micelles. Afterwards, the mixture was mildly vortexed and allowed to equilibrate. In the systems with polypeptides, the solution of polypeptide with liposomes or micelles was prepared first and then BR was added.

For the VCD measurements, the BR concentration was 5 or 7×10^{-2} M. The PLAG concentration was 6.5 g/L, which represented the molar concentration of 4.2×10^{-2} M per amino-acid residuum. The concentration of the lipids was 1.4×10^{-1} M and that of SDS was 5.6×10^{-1} M. The small signals measured in VCD cause that an optimal energy throughput on a detector is needed which represents the desirable entire absorption in the IR region of measured solutions of A ~ 0.4. This fact prohibits extending the concentration range in several orders by an increase of the path length because this simultaneously increases the absorption of solvent and significantly decreases the energy throughput [43,44].

For the ECD measurements, the BR concentration was in the broad range of 1×10^{-5}–5×10^{-2} M. The highest concentration corresponded to the concentration used for the VCD measurements and enabled the comparison between both techniques. The PLAG concentration was 6.4×10^{-4} M. The concentration of DMPC and SPM was given by the desired ratios of the component. The concentration of DMPG and DPPG was 2.8×10^{-3} M and that of SDS 1.1×10^{-2} M.

For the fluorescence emission measurements, the BR concentration was 1×10^{-5} M, the concentration of the DMPC and SPM liposomes was 1×10^{-3} M, and HSA concentration was 1×10^{-5} M.

All measured solutions did not show presence of aggregates or precipitates as was confirmed by their centrifugation. The aggregation was observed for pH > 8 and prevented the spectral measurements in the broader range of pH.

2.4. Vibrational circular dichroism and transmission Fourier transform infrared spectroscopy

The VCD and IR absorption spectra in the 1800–1400 cm^{-1} region were measured on a FTIR IFS 66/S spectrometer equipped with a PMA 37 VCD/IRRAS module (Bruker, Germany).

The samples were placed in a demountable cell (A145, Bruker, Germany) composed of CaF_2 windows separated by a 23 μm Teflon spacer that was suitable for the concentrations used. All of the VCD spectra were recorded at a spectral resolution of 8 cm^{-1} and are the average of the 15 blocks of 3686 scans (20 min). The OPUS 6.5 software (Bruker, Germany) was used for the VCD spectra calculations. The VCD and IR spectra were corrected for a baseline, which was obtained as a spectrum of the buffer measured under the same experimental conditions. The composition of the mixture of deuterated and non-deuterated phosphate buffer used as a solvent for the baseline correction corresponded to the H to D exchange during the extrusion and was obtained from the IR absorption spectra.

The temperature dependence of the spectra was measured in a demountable electric heated cell P/N20500 (Specac, UK) constructed of the CaF2 windows separated by a 23 μm Teflon spacer. A heated jacket controller 3000 series (Specac, UK) adjusted the temperature.

2.5. Electronic circular dichroism, fluorescence emission spectroscopy and absorption in the ultraviolet and visible region

The ECD, fluorescence emission and UV–vis absorption spectra were measured on a J-810 spectrometer equipped with a fluorescence accessory FDCD-404 L (Jasco, Japan). The ECD and UV–vis absorption spectra were measured in a quartz cuvette with an optical path length of 1 cm, 1 mm, 0.5 mm, 100 μm and 10 μm (Starna, USA) and the fluorescence emission spectra in a quartz cuvette with an optical path length of 1 cm (Helma, Germany). The conditions of the ECD and UV–vis absorption measurements were as follows: a spectral region of 200–600 nm, a scanning speed of 5 nm/min, a response time of 16 s, a resolution of 0.5 nm, a bandwidth of 1 nm and a sensitivity of 100 mdeg. The final spectrum was obtained as an average of 8 accumulations. The spectra were corrected for a baseline by subtracting the spectra of the corresponding buffer. The conditions of the fluorescence emission measurements were as follows: a spectral region of 460–800 nm, excitation wavelength 435 nm, a response time of 2 s, a resolution of 1 nm, a bandwidth of 10 nm and a sensitivity of 900 V. The final spectrum was obtained as an average of 5 accumulations. All the measurements were conducted at room temperature (25 °C).

3. Results and discussion

3.1. Bilirubin interaction with zwitterionic liposomes

The previously published ECD studies of the interaction between BR and liposomes have shown that BR is enantioselectively recognized by the liposomes of a certain composition [6,15]. The ECD spectral features were typical of the P-form of BR. However, the ECD spectra can bring only information on the BR part of the molecular system. No information about the lipid part of the system could be obtained. The VCD method, which we employed, is closely related to IR method and does not depend on the UV–vis chromophores and may describe both of the components of the system.

We studied the interactions between the BR and the zwitterionic liposomes composed of DMPC, a lipid similar to the lipids of usual cell membranes. In a solution, BR exists as a racemic mixture of two rapidly interconverting enantiomers with P- and M-forms. Therefore, although the pattern with local maxima localized at 1617 cm^{-1} and 1557 cm^{-1} was observed in the IR spectrum for the BR solution (Fig. 1A), no VCD signal was observed for the racemate. The IR band with the maximum at 1617 cm^{-1} is broad and the second derivative analysis showed that another two bands at 1650 and 1630 cm^{-1} were overlapped by a band of higher intensity. The band at 1617 cm^{-1} was assigned to pyrrole ring deformation in a molecule with hydrogen bonds, the band at 1630 cm^{-1} was assigned to vinyl coupled lactam and pyrrole ring stretching vibrations and the band at 1650 cm^{-1} was assigned to the stretching C═O vibration [45,46]. The band at 1557 cm^{-1} also consisted of several signals: pyrrole C═C, N – H and lactam C – N stretching vibrations at 1545 cm^{-1} and an asymmetric COO− stretching vibration at 1557 cm^{-1}.

Despite the chiral center in the DMPC molecule (for structure see Fig. S1), the solution of the DMPC liposomes also had no observable VCD signal (Fig. 1A). Without additional chiral agent, the conformational diversity of the long non-rigid lipid chains diminished the optical activity of the chiral center and caused observed weak signal of the liposomes. A lipid signal in the studied IR region localized at 1735 cm^{-1} was assigned to the C═O lipid groups. For the solution of BR with DMPC liposomes, several VCD signals were observed (Fig. 1A): a negative couplet localized at 1643(−)/1680(+) cm^{-1} corresponding to the IR peak at 1650 cm^{-1} and a negative VCD signal at 1743 cm^{-1} corresponding to the IR signal at the same position. Interestingly, the IR spectra were stable in the time domain, while the intensity of the VCD signal at 1743 cm^{-1} increased and a new negative signal localized at 1567 cm^{-1} was observed with time. The VCD pattern of BR/DMPC reached its stable shape in six hours and became stable for tens of hours.

The IR and VCD peaks in the mutual solution of both BR and DMPC were assigned based on the spectra measured for the compounds themselves. The negative VCD band at 1743 cm^{-1} was assigned to the C═O groups of DMPC [45]. The negative couplet localized at 1643(−)/1680(+) cm^{-1} was assigned to the stretching vibration of the C═O groups of BR. The negative signal at 1567 cm^{-1} was assigned to the IR peak at 1557 cm^{-1} of an antisymmetric COO^- stretch and previously was used as a marker for BR helicity [33–35]. According to these previous results, the negative sign of this band was assigned to the M-form of BR, which suggested that BR was recognized by the chiral DMPC liposomes also in the M-form.

The previously published study [6] concluded that BR bound to the DMPC membrane in its P-form, which was based on the observation of a positive BR couplet in the ECD spectra for a BR concentration of 10^{-5} M. To explore the discrepancy between our VCD findings at the BR concentration 5×10^{-2} M and ECD results at concentration of 10^{-5} M, we measured the ECD and UV–vis spectra of the BR/DMPC solutions in the broad concentration range of BR: 1×10^{-5}–5×10^{-2} M and documented their concentration dependence. The positive couplet observed at 1×10^{-5} M was converted to a more complex spectral form with the concentration increase. For the high concentrations unusual for the ECD measurements of BR, a negative couplet was observed as a main spectral feature (Fig. 2A) confirming that at higher BR concentrations in the presence of DMPC, BR preferentially existed in its M-form. A significant blue shift was observed in the UV–vis spectra for high concentrations. As Person et al. [47] suggested, the intensity of the higher energy transition in the UV–vis would be increased for a

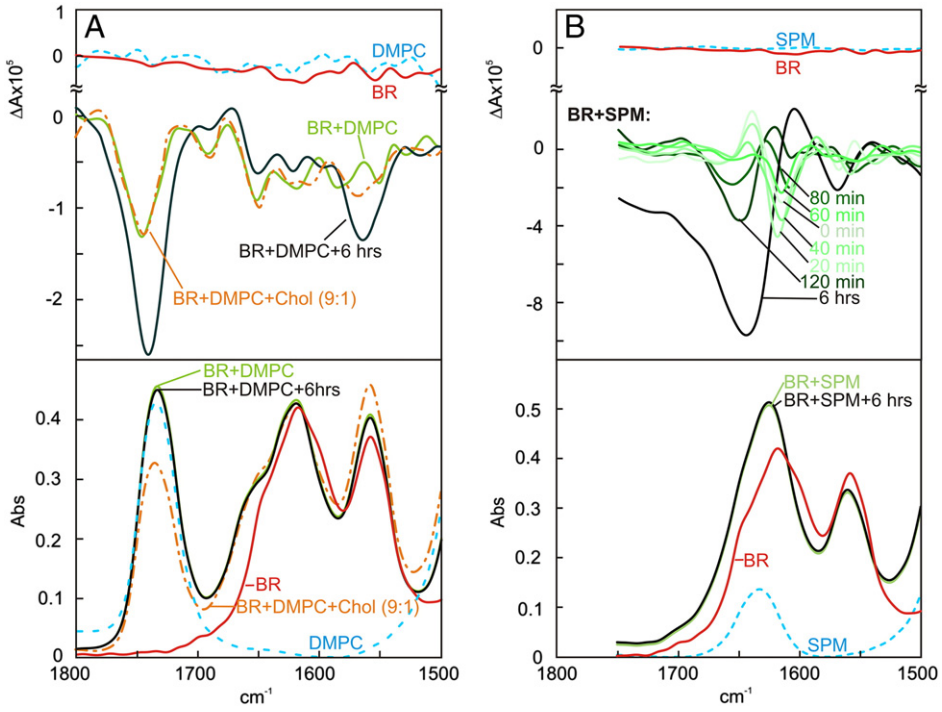

Fig. 1. A. The VCD (top) and IR (bottom) spectra of the DMPC liposomes (dashed), BR and of the BR with the DMPC liposomes 20 min after sample preparation and 6 h after sample preparation, and BR with DMCP liposomes with 10 mol% of cholesterol. ($c_{BR} = 5 \times 10^{-2}$ M, $c_{DMPC} = 1.4 \times 10^{-1}$ M, $c_{DMPC\ +\ Cholesterol} = 1.4 \times 10^{-1}$ M). B. The VCD (top) and IR (bottom) spectra of the SPM liposomes (dashed), BR and the spectral changes over time for a BR solution with the SPM liposomes. ($c_{BR} = 5 \times 10^{-2}$ M, $c_{SPM} = 1.4 \times 10^{-1}$ M).

more closed porphyrin-like BR conformation, which is high in energy (~20–30 kcal/mol above the isoenergetic global minimum energy conformations), so the UV–vis spectral pattern should be blue-shifted, and the ECD intensity would be significantly decreased, which was observed (Fig. 2A) as the observed negative couplet had low intensity. Although the suspected porphyrin-like M-form of bound BR at high concentration would be quite high in energy, it is possible that it was stabilized by the DMPC membrane. It should be noted that it is not possible to measure the VCD spectra for lower concentrations as was described in paragraph 2.3. However, the obtained ECD results indicated that BR bound to the

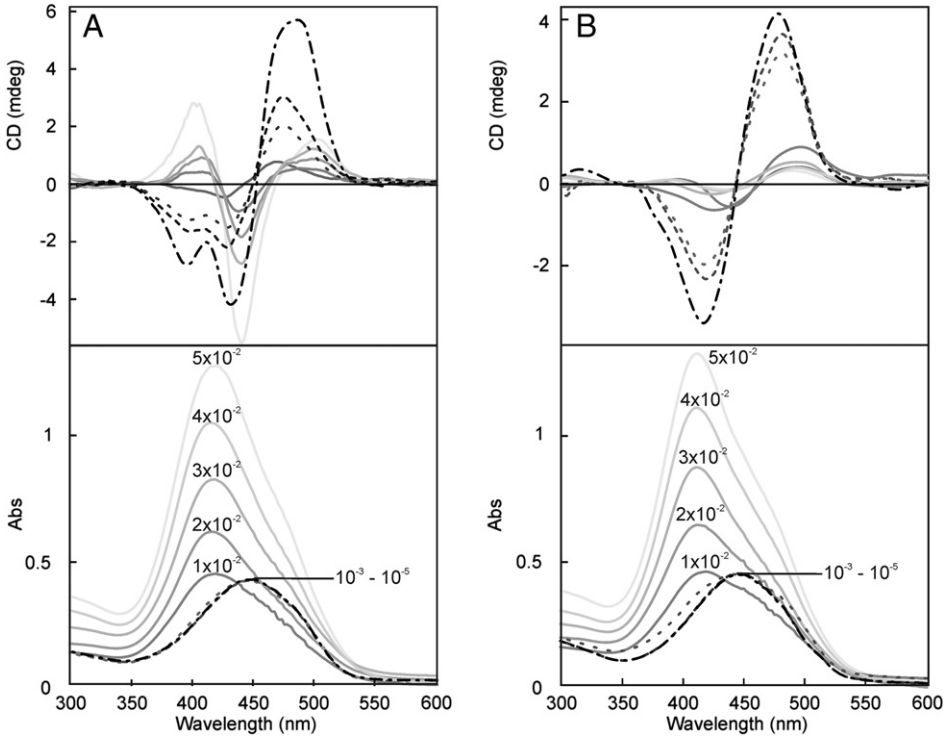

Fig. 2. The ECD spectra of BR with the DMPC liposomes (A) and with the SPM liposomes (B) in the concentration range of BR: 10^{-5} M (a 10 mm cuvette, dot-and-dash line), 10^{-4} M (a 1 mm cuvette, dashed line), 10^{-3} M (a 10^{-1} mm cuvette, dotted line), 10^{-2}–5×10^{-2} M (a 10^{-2} mm cuvette, solid lines, concentrations in M are denoted in the spectra). The concentration of DMPC and SPM was in the range 1×10^{-3}–1.4×10^{-1} M. The ratio of BR and lipid was adjusted to optimized conditions for the measurement and was in the range 0.01 for low concentrations and 0.35 for high concentrations.

DMPC membrane in a P-form up to a concentration of 1×10^{-4} M of BR and predominantly in the M-form at higher concentrations (Fig. 2A). Besides the negative couplet, a positive couplet localized at the low energy side of the BR absorption band was observed as well in the ECD spectra for high concentrations of BR. This indicated that part of the BR was bound also in the P-form. For all the measured BR concentrations, a shoulder at ~507 nm was observed in the UV–vis absorption spectra indicating that a part of BR was in the colloidal state [48,49] which reflected a low solubility of BR in an aqueous solution. Nevertheless, the measured intensity of the ECD spectra demonstrated that the major part of BR participated in diastereoisomeric interactions.

In this study, the VCD spectra were also used to follow the lipid part of the system. In the presence of BR, a new VCD signal was observed at 1743 cm^{-1} assigned to the C═O groups of the lipid. This indicated that these groups, which were close to the lipid chiral center, were influenced by the interacting BR. Because the C═O groups of the lipid were not localized on the surface of the bilayer, we may assume that BR entered into the bilayer closely to the C═O lipid groups. This was also observed in a former IR absorption study [25]. However, the VCD spectra revealed the influence of BR on the C═O region of DMPC, which had not been observed before. Observed VCD signal assigned to the lipid part documented that chiral discrimination of BR decreased the conformational diversity of the lipids documented by non-measurable optical activity of alone lipids in the solution.

The interaction of BR with the DMPC liposomes was observed also by the fluorescence emission spectroscopy (Fig. 3). The strong quenching prohibited the measurement of the BR fluorescence in the phosphate buffer solution; therefore a spectrum of BR interacting in the primary binding site of HSA [48] was used in the comparison with the spectra of BR in the liposomal solutions. Fig. 3 shows that within the spectral resolution the position of the emission maxima of the BR solution with the DMPC liposomes was the same as in the solution with HSA. This indicated that BR interacting with the DMPC bilayer was in a similar environment as when bound to HSA, i.e. less polar than water [50], and therefore probably buried in the bilayer.

The VCD and ECD spectra indicated that BR was recognized by the membrane in different chiral forms depending on its concentration and its spatial form was probably changed during the interaction, which was also confirmed by the fluorescence emission and UV–vis spectra. Similar behavior of BR has been observed before [15] for BR in different a model system consisting of a single layer and was explained as the inducement of a different organization of aggregates or a different site of binding of BR because of concentration changes. According to our VCD and ECD observation for the bilayer system, a significant part of BR entered the bilayer and at its lower concentrations preferred the P-form. At higher concentrations, restrictions in the bilayer arose (higher BR/lipid ratio) and BR was forced to take more flat porphyrin-like conformation in the M-form, influenced also by the chiral center of the DMPC lipids which is located closely to the C═O groups in the molecule (Fig. S1 in Supporting material). The time changes which were observed in the VCD of the lipid part of the system and also in the negative BR band at 1567 cm^{-1} (antisymmetric COO^- stretch) which indicated the M-form, confirm this suggestion. As the IR spectra were stable in terms of time, the changes in the VCD spectra were caused by the reorganization of the bilayer in the presence of BR. The time changes were also observed in the ECD spectra for the BR part at lower concentrations of BR (Fig. S2). After the BR interaction with the bilayer occurred, the lipids probably slowly organized (over hours) in order to arrange the BR molecules, which was connected to the observed VCD pattern.

SPM is one of the most common lipids that occur in neural cell membranes. The solution of the SPM liposomes had only one IR band in the studied region localized at 1632 cm^{-1} which was assigned to the C═O vibration (Fig. 1B). The IR spectrum of BR alone was described above. The solution of BR with the SPM liposomes had several IR and VCD signals (Fig. 1B). The IR spectra were stable over time and two broad bands with maxima localized at 1628 and 1562 cm^{-1} were observed. However, the VCD signal changed quite rapidly during the measurement (one spectrum was measured for 20 min) as shown in Fig. 1B: for the fresh mixture, a negative couplet localized at 1614(−)/1637(+) cm^{-1} was observed and this gradually changed to a positive couplet localized at 1608(+)/1649(−) cm^{-1}. In addition, a negative signal localized at 1572 cm^{-1} was observed. These newly formed signals were stable for tens of hours.

The ECD and UV–vis spectra shown in Fig. 2B indicated concentration dependence in the region of the BR signal: for the concentration of 10^{-5} M, previously used in [6], a positive couplet was observed indicating the P-form of interacting BR (centered at 442 nm, Fig. 2B). For the same concentrations and conditions as used for VCD (5×10^{-2} M, Fig. 2B), a low intensity positive couplet was observed as well but at a slightly different position (centered at 460 nm). The observed ECD signal is typical for the overlapped positive and negative couplets, meaning that the observed positive couplet was complemented by a low intensity negative couplet at higher energy. The UV–vis spectra also differed for the low and high concentrations. The high energy part of the absorption band localized at 412 nm became more intensive than the low energy one at 450 nm compared to the spectra measured for low concentrations.

We assume that the changes over time in the VCD spectra of BR/SPM system and their reason were analogous to the BR system with DMPC liposomes. The signal intensities for BR with the SPM liposomes were approximately three times higher than in the case of the BR with the DMPC liposomes. A negative couplet of lower intensity overlapped by the previously discussed VCD signals of stronger intensity was observed at 1656(−)/1672(+) cm^{-1} in the BR/SPM system (Fig. S3 in Supplementary material). The position of this couplet is nearly the same as the negative couplet at 1643(−)/1680(+) cm^{-1} for the BR/DMPC liposomes system. The shape of this signal is the same over the course of time, with the exception of the last spectrum where the overlapping signal at 1608(+)/1649(−) cm^{-1} is so strong and wide that it made observation of the less intense BR signal impossible. Hence, the spectral shape that changed over time (to 1608(+)/1649(−) cm^{-1}) was preferentially assigned to SPM, which was slowly reorganized because of the presence of BR, with the possible minor contribution of BR. The negative band at 1572 cm^{-1} was in the region of BR absorption and was assigned to BR. However, it is overlapped by the intensive couplet at 1608(+)/1649(−) cm^{-1} and this and the overlapping couplets in the ECD spectrum made it impossible to determine the conformation of the bound BR.

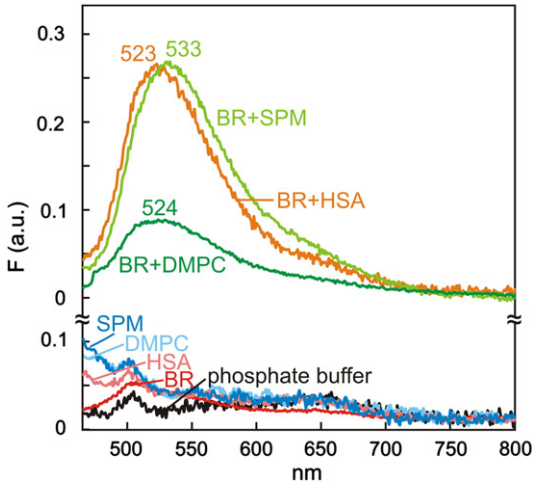

Fig. 3. The fluorescence emission spectra of BR with the DMPC liposomes, BR with the SPM liposomes and BR with HSA (top), and of BR, HSA, the DMPC liposomes, the SPM liposomes and phosphate buffer (bottom). ($c_{BR} = 1 \times 10^{-5}$ M, $c_{DMPC} = 1 \times 10^{-3}$ M, $c_{SPM} = 1 \times 10^{-3}$ M, $c_{HSA} = 1 \times 10^{-5}$ M).

The assignment of the other VCD signals to the IR peaks and to the functional groups of either SPM or BR was more complex for the system with the SPM liposomes than that with the DMPC liposomes. The IR peaks of the C═O groups of SPM and BR strongly overlapped and this made the assignment of the VCD bands ambiguous. However, the intensity of the induced VCD signal was about three times higher for the BR/SPM than for the BR/DMPC system. Note the different scale used for the VCD spectra in Fig. 1. These observations implied that BR formed a stable associate with both the liposomes and that this complex did not decompose over time. Moreover, the BR/SPM associate appeared robust because the induced VCD signal showing the mutual influence of BR and SPM was very strong. When compared to the DMPC liposomes, the SMP liposomes showed a significantly stronger impact of BR on the membrane structure which may be connected to the neurotoxicity of BR.

The fluorescence emission spectrum of BR with the SPM liposomes (Fig. 3) was red shifted compared with the spectra of BR interacting with the DMPC liposomes or interacting in the primary binding site of HSA. This suggests that BR was probably bound in a more polar environment and therefore was located closer to the surface of the SPM liposomes than of the DMPC liposomes.

It should be noted that the VCD signal of BR for the stretching C═O vibration localized at 1643(−)/1680(+) cm^{-1} and at 1656(−)/1672(+) cm^{-1} for BR/DMPC liposomes and BR/SPM, respectively, (Fig. 1 and Fig. S3 in Supplementary material) did not change over time, while the signals at 1557 and 1572 cm^{-1} for the BR/DMPC liposomes and BR/SPM liposomes, respectively, changed manifestly. These observations and the fact that the C═O liposome bands at 1743 cm^{-1} and at 1614(−)/1637(+) cm^{-1} changed over time as well suggested that the changing bands of BR belonged to BR groups that were strongly affected by the liposomes, mainly COO^-, and their changing VCD signal might be result of their chiral orientation induced from the lipids. Hence, the non-changing signals of BR were probably connected to its inherent chirality that arose from the structural arrangement.

3.1.1. Influence of cholesterol

Cholesterol is a very important and vital part of human cell membranes. It mainly fulfills the role of a membrane strengthener. Hence we prepared the liposomes composed of 0-10 mol% of cholesterol and of DMPC. The size of these liposomes was about 30% bigger ((130 ± 4) nm) than without cholesterol because the particles were more robust and so even larger particles were able to penetrate through 100 nm pores of the membrane during the extrusion.

However, the VCD (Fig. 1A) and also the ECD spectra (results not shown) of BR with liposomes containing cholesterol did not differ from the spectra with liposomes composed only of DMPC. Even the cholesterol bands in the IR did not change in the presence of BR. Hence we may assume that BR preferred the interaction with DMPC over cholesterol. However, the changes in the range of hours were not observed in these systems unlike the liposomes without cholesterol. This may have been due to the strengthening properties of cholesterol. The lipids in liposomes were probably not able to rearrange over time as was observed for the DMPC without cholesterol and SPM liposomes.

3.1.2. Influence of pH and temperature

As the physiological conditions may differ from those in the laboratory, we investigated the influence of pH and temperature on the BR systems with the DMPC and SPM liposomes. Especially the effect of pH on these systems is very important, because acidosis may strongly influence the BR interaction with membranes [7].

Both types of the studied liposomes with BR had a very strong response to pH changes. As shown in Fig. 4 (See Fig. S4 in Supplementary material for the ECD spectra), the decrease of pH from pH 7.5 to pH 6 caused a decrease of the VCD signal, while the IR absorption spectra remained unchanged. At pH 6, the observed signals were very weak and determined the lower limit of the used pH range. The VCD signal also decreased in the case of increasing pH. Only spectra up to pH 8 were measurable, because the system aggregated above pH 8 and we were not able to measure the aggregated suspension. Detailed pH changes showed that both the systems were invariable (the VCD signals did not change) from pH 7.3 to 7.6.

The pH changes were probably caused by BR ionization dependence on pH. As there is a constant debate in the literature on the pKa values of BR [51–54], which strongly depend on the solution environment, we were not able to use the precise values. However, it is probable that BR was non-charged at lower pH and had two negative charges at higher pH. The non-charged BR probably did not interact with zwitterionic liposomes. On the other hand, the doubly charged BR may have worked as a bridge between two liposomes and that is why the system aggregated and the spectra were not measurable for higher pH. The pH dependence suggested that only the singly charged molecules may interact with the bilayer.

The solution pH influenced the time dependence of the VCD spectra. For the DMPC liposomes with BR, the C═O lipid signal did not change with time outside the pH interval 7.3–7.6. The VCD spectrum intensity was low and stable over time. On the other hand, for the SPM liposomes with BR, the signal increased over time but it did not reach the intensity observed for pH from 7.3 to 7.6. Hence, the system with the DMPC liposomes was more sensitive to pH and the lipids did not rearrange to form a highly ordered system characterized by a strong VCD signal. In the more robust system with the SPM liposomes, BR interacted with the bilayer and influenced its VCD signal in nearly same manner as at pH 7.5.

We observed that even slight changes in pH strongly influenced the BR binding to the model membranes.

The effect of temperature on the studied systems (Fig. 5, Fig. S5 in Supplementary material for the ECD spectra) reflected the melting temperature of the bilayers which is below 25 °C for DMPC and slightly above 40 °C for SPM. For BR with the DMPC liposomes, the VCD signal measured at 15 °C, i.e. below the temperature of the phase transition, was weak. It significantly increased at 25 °C and then gradually decreased with increasing temperature, but the signal was measurable even at 70 °C. For the BR with the SPM liposomes, the VCD signal slightly increased when the temperature was increased up to 40 °C where the phase of the membrane is changed and then it also started decreasing for higher temperatures up to 70 °C. Interestingly, the temperature changes were reversible in both the systems. When we cooled them down to 25 °C, the initial signals were restored. Our VCD measurements showed a surprisingly high stability of BR interacting with the studied membranes which was not observed for the BR solutions. The temperature reversibility was confirmed also by the ECD measurements (Fig. S5 in Supplementary material).

The spectral changes dependent on the temperature clearly reflected the melting temperatures of the bilayers for the both studied systems. From 15 to 25 °C (25 to 40 °C for SPM), the VCD signal of DMPC slightly increased because the membrane became more flexible but it was still quite rigid and so it was able to accommodate more BR molecules. The DMPC bilayer melted above 23 °C (40 °C for SPM) and this phase change probably caused a bigger flexibility and a fluidity of the whole system and BR was again bound less strongly in such free surroundings. Because of this, the observed VCD signal decreased in both the studied systems.

The signals were restored in both systems after the decrease of the temperature to 25 °C which indicated that the temperature variation in the range of 25–70 °C did not hamper the BR-liposome interactions. Even the DLS measurement of the liposome size distribution confirmed that as with the liposomes alone, the size distribution of the liposomes in the presence of BR was not strongly influenced by the temperature changes.

3.2. Bilirubin-model membrane with bound polypeptide

The BR interaction with membranes might be influenced by the presence of membrane proteins which either penetrate throughout

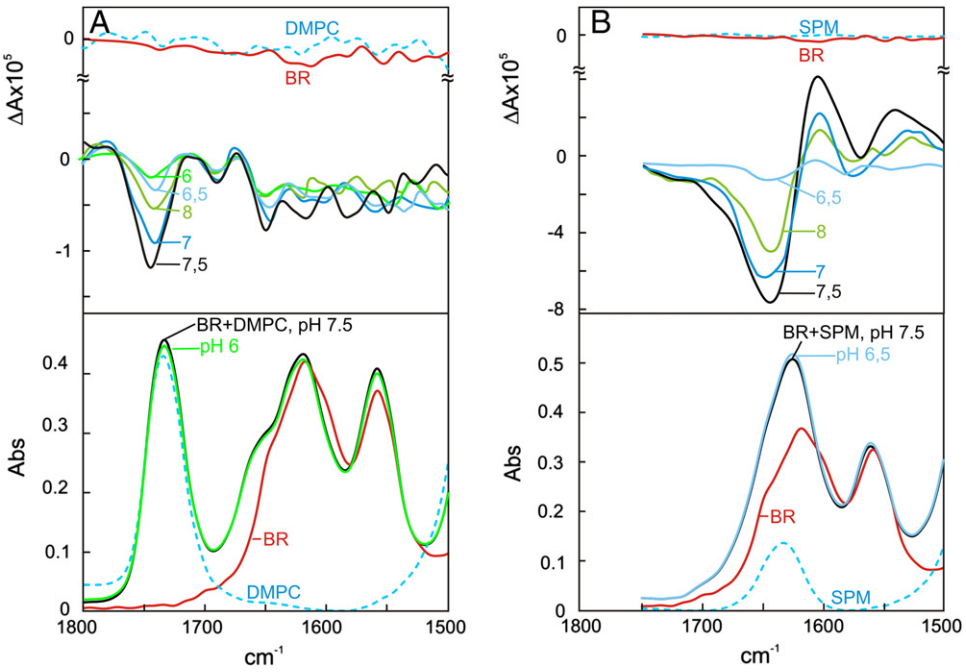

Fig. 4. A. The VCD (top) and IR (bottom) spectra of the DMPC liposomes (dashed), BR and the BR with the DMPC liposomes for different pH. ($c_{BR} = 5 \times 10^{-2}$ M, $c_{DMPC} = 1.4 \times 10^{-1}$ M). B. The VCD (top) and IR (bottom) spectra of the SPM liposomes (dashed), BR and the BR with the SPM liposomes for different pH. ($c_{BR} = 5 \times 10^{-2}$ M, $c_{SPM} = 1.4 \times 10^{-1}$ M).

the membrane or are bound to its surface. In this study, we focused on the second case, which is more probable to influence the BR interaction with the membrane, as BR may prefer to bind to the polypeptide instead.

As a model for the membrane proteins, synthetically prepared PLAG was chosen. This polypeptide has served previously as an appropriate model for antimicrobial α-helical peptides [55]. We have shown [36] that PLAG binds to the negatively charged model membranes in the *α-helical* structure while it takes the *polyproline II*-like conformation (also called random coil) in the plain solution of a phosphate buffer. Previously, we observed that BR was able to bind to the polypeptide in the *α-helical* conformation and did not bind to the *polyproline II*-like polypeptide [34]. Negatively charged model membranes, liposomes composed of DMPG or DPPG and micelles composed of SDS, were chosen, because BR does not tend to bind to such membranes as it has a negative charge as well. Two negatively charged lipids of different

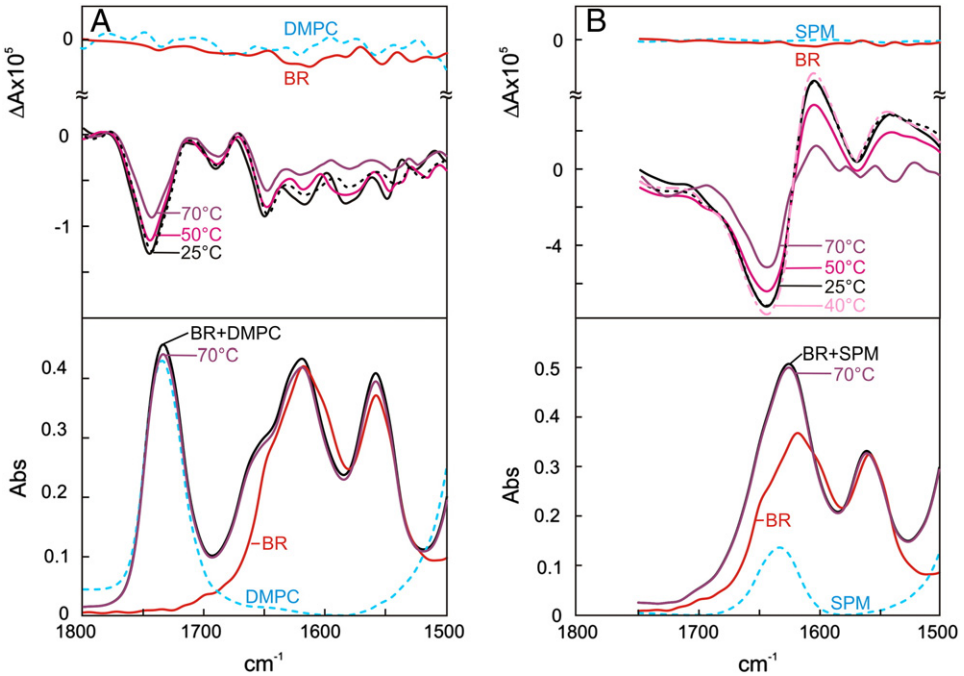

Fig. 5. A. The VCD (top) and IR (bottom) spectra of the DMPC liposomes (dashed), BR and the BR with the DMPC liposomes for different temperatures. The dashed line depicts the system after a cool down to 25 °C. ($c_{BR} = 5 \times 10^{-2}$ M, $c_{DMPC} = 1.4 \times 10^{-1}$ M). B. The VCD (top) and IR (bottom) spectra of the SPM liposomes (dashed), BR and the BR with the SPM liposomes for different temperatures. The dot-and-dash line depicts the increased signal after the increase of the temperature to 40 °C. The dashed line depicts the system after a cool down to 25 °C. ($c_{BR} = 5 \times 10^{-2}$ M, $c_{SPM} = 1.4 \times 10^{-1}$ M).

hydrocarbon chain length were used in this study. The DMPG was of the same length as DMPC in the first part of the study and DPPG was used as a connection to our previous study of polypeptide interactions with liposomes [36]. The results obtained for these two model membranes did not show a dependence on the hydrocarbon chain length.

Fig. 6 (see Fig. S6 in the supplementary material for the DPPG results) shows the VCD and IR absorption spectra of different molecular systems composed of BR, the DMPG liposomes, and PLAG. In the IR spectra, a band at 1736 cm^{-1} was assigned to the stretching C═O vibration of DMPG. Several bands localized at 1658, 1644, 1607 and 1588 cm^{-1} assigned to PLAG were observed and were slightly shifted in the presence of the DMPG liposomes and localized at 1644, 1634, 1603 and 1582 cm^{-1}. No VCD signal was observed in the solution of BR, because it was a racemic solution, and in the solution of DMPG liposomes, because of conformational diversity in the vicinity of the chiral center (Fig. 6A, Fig. S6 for the DPPG results). For the solution of PLAG alone, a negative VCD couplet was observed in the region of Amide I localized at 1663(+)/1637(-) cm^{-1} which was complemented by a positive signal localized at 1607 cm^{-1}, and the same was observed also in the solution of PLAG with BR (Fig. 6A). The negative couplet observed for the PLAG solution and BR/PLAG solution was typical of the *polyproline II*-like conformation [56–59]. The presence of BR did not influence the PLAG structure and no chiral recognition of BR was observed in this secondary system. For PLAG with DMPG liposomes, the VCD signal significantly changed and three VCD peaks at 1660(−)/1644(+)/1624(−) cm^{-1} were observed and clearly reflected the *α-helical* conformation [56,57] with a small fraction of *polyproline II*-like conformation.

The ECD spectra in Fig. 7A (see Fig. S7 for the DPPG results) confirmed the effect of negatively charged liposomes on the structure of PLAG: the spectrum of the PLAG solution with a weak positive signal at 216 nm and an intensive negative signal at 200 nm, typical of the *polyproline II*-like conformation, was converted with the addition of the DMPG liposomes to two negative signals at 207 and 223 nm and a positive signal localized below 200 nm, indicative of a significant content of the *α-helical* conformation. The presence of BR did not change the typical *α-helical* shape of the ECD spectra of the PLAG with DMPG.

In the region of the BR absorption (~350–550 nm), no ECD signal was observed for the PLAG/DMPG (Fig. 7B, Fig. S7 for the DPPG results). However, after the addition of BR to this system, an ECD signal was observed also in this region 403(−)/453(+)/508(−) nm which indicated the binding of BR.

Fig. 6B shows the VCD and IR spectra of the BR/PLAG/DMPG ternary system. A broad negative VCD signal at 1754 cm^{-1} was observed in the region of DMPG absorption (two resolved signals were observed for DPPG, Fig. S6). The amide I region was completely different from that observed for the BR/PLAG or PLAG solutions. Two negative signals at 1659 and 1627 cm^{-1} were observed which probably resulted from the superposition of the BR and PLAG signals. As the ECD spectra of the BR/PLAG/DMPG solution clearly indicated that BR is diastereoisomerically bound in this system (Fig. 7B), we expected that BR contributed to the observed VCD signal of the BR/PLAG/DMPG ternary system. The estimation of the VCD induced by interactions in the ternary system was obtained when we subtracted the PLAG/DMPG solution VCD spectrum from the VCD spectrum of the BR/PLAG/DMPG solution (Fig. 6B). We could not be certain of the PLAG and DMPG spectral pattern, which may have changed after the addition of BR into the solution. However, the ECD did not show any changes in the spectral pattern typical of the α-helix after the addition of BR into the solution. So, we assumed that the PLAG structure did not change significantly, may be spectrally subtracted and that the resulting difference spectrum came mainly from BR in the region

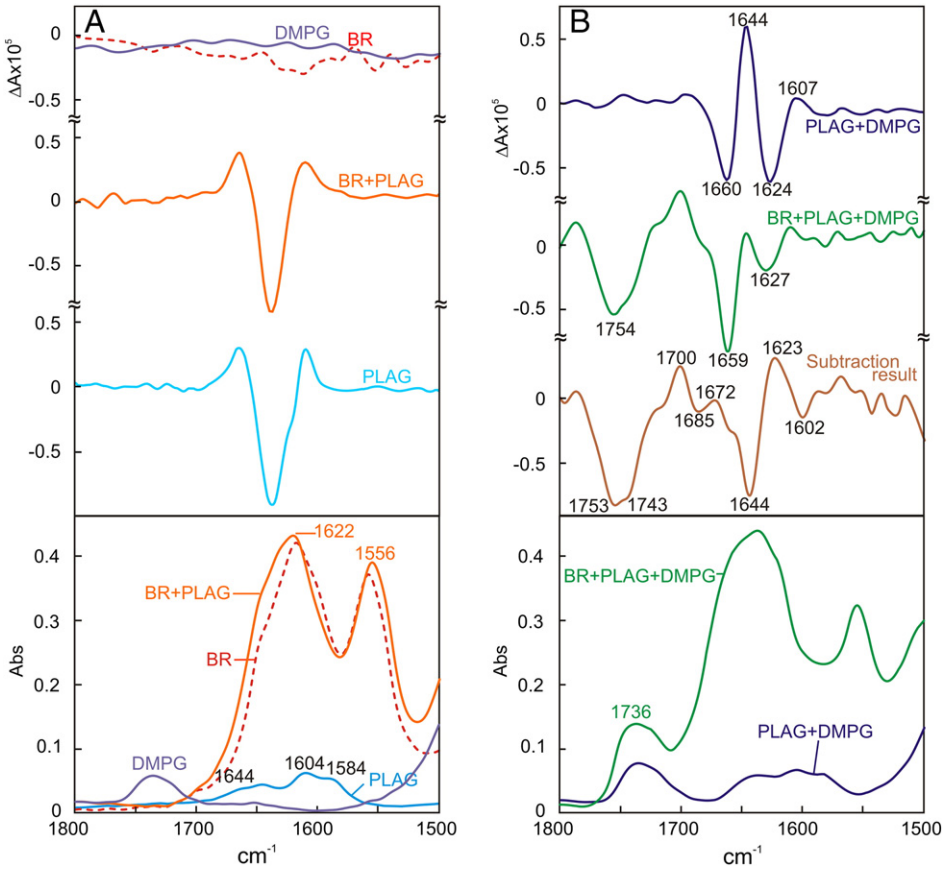

Fig. 6. A. The VCD (top) and IR (bottom) spectra of DMPG liposomes, BR (dashed line), PLAG and BR with PLAG. B. The VCD (top) and IR (bottom) spectra of PLAG with DMPG liposomes, BR with PLAG and DMPG liposomes, the difference spectrum of BR with PLAG and DMPG liposomes minus PLAG with DMPG liposomes (dashed line). ($c_{BR} = 7 \times 10^{-2}$ M, $c_{PLAG} = 4.2 \times 10^{-2}$ M, $c_{DMPG} = 1.4 \times 10^{-1}$ M).

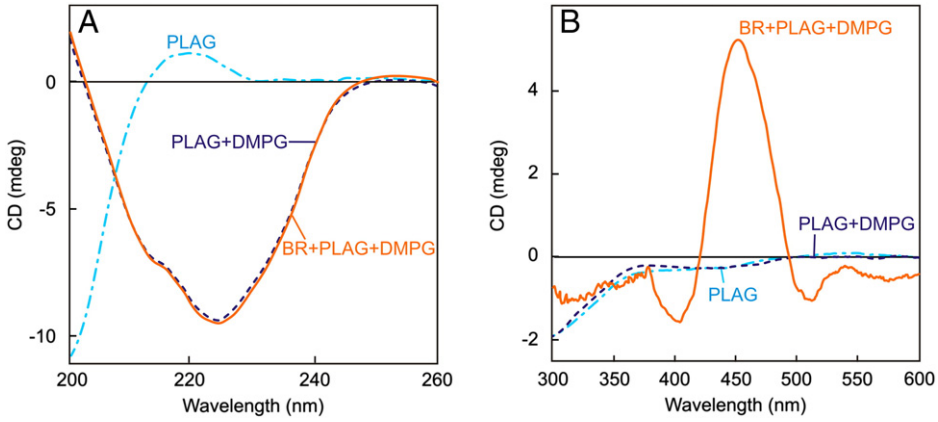

Fig. 7. A, B. The ECD spectra of PLAG (dot-and-dash line), PLAG with DMPG liposomes (dashed line) and BR with PLAG and with DMPG liposomes (solid line) in the spectral regions typical of PLAG (A) and BR (B). ($c_{BR} = 1 \times 10^{-5}$ M, $c_{PLAG} = 6.4 \times 10^{-4}$ M, $c_{DMPG} = 2.8 \times 10^{-3}$ M).

of the BR IR absorption (1700–1600 cm^{-1}) and from DMPG in the region around ~1750 cm^{-1} typical of DMPG absorption: We assigned the VCD signals at 1685, 1644, 1623 and 1602 cm^{-1} to the bound BR reflecting the C═O stretching and pyrrole ring stretching and deformation vibration which overlap in this region [33–35,45,46]. The negative VCD signal localized at 1743 cm^{-1} was assigned to DMPG corresponding to the absorption band at 1736 cm^{-1}. The VCD signal at 1753 cm^{-1} was assigned to DMPG corresponding to the weak absorption which was overlapped by the 1736 cm^{-1} signal. Hence, we documented that the spatial arrangement of DMPG in liposomes was influenced by the presence of BR, although it is not probable that BR would bind directly to DMPG because of the opposite charges of these two compounds. It should be noted that the presence of PLAG alone did not induce the VCD in the region that is characteristic of DMPG (Fig. 6B).

The VCD spectral results and also the ECD spectra (Figs. 6 and 7) showed that BR took part in the interaction in the BR/PLAG/DMPG ternary system. The observed signals did not indicate in either VCD or ECD whether only the P- or M-form of BR bound to the PLAG, rather they documented the variety of the structural forms of BR bound in the studied ternary system. Analogical results were obtained also for the DPPG liposomes (supplementary material) indicating a preference of BR interaction with PLAG.

The VCD and IR spectral results obtained for the BR/PLAG solution with the SDS micelles are shown in Fig. 8. No VCD signal was observed for the solutions of BR and of the SDS micelles. For the PLAG/SDS micelles system, the observed VCD signal in the amide I region localized at 1662(−)/1647(+)/1620(−) cm^{-1} was similar to the PLAG/DMPG system reflecting the *α-helical* conformation [56,57] with a few remnants of *polyproline II*-like conformation. This was also confirmed by the ECD spectra shown in Fig. 9A, where the spectrum of PLAG with the SDS micelles had two negative bands at 208 and 227 nm and tended towards a positive signal under 200 nm, which are the ECD spectral features characteristic of *α-helical* conformation. In the IR spectra, peaks localized at 1642, 1633, 1604 and 1584 cm^{-1} were observed.

In the region of the BR absorption (350–550 nm), again no ECD signal was observed for the PLAG/SDS micelles solutions (Fig. 9B). However, after the addition of BR to this system, an ECD signal was observed at 431(+)/483(−)/541(+) nm indicating the diastereoisomeric interaction of BR.

For the BR/PLAG/SDS micelles system, negative VCD signals localized at 1656, 1629, 1560 and 1530 cm^{-1} were observed. For an estimation of the BR contribution, we subtracted the VCD spectrum of PLAG/SDS from that of the BR/PLAG/SDS system (Fig. 8). In the difference spectrum, two distinct negative signals were observed localized at 1643 and 1560 cm^{-1}. The negative signal at 1560 cm^{-1} indicated the M-form of BR, which was also confirmed by the ECD spectra (Fig. 9B). A similar result was also observed previously for BR in the system with PLAG and dodecanoate micelles [34].

The study of BR in ternary systems with PLAG and liposomes or micelles has shown that in the presence of PLAG, a model of membrane

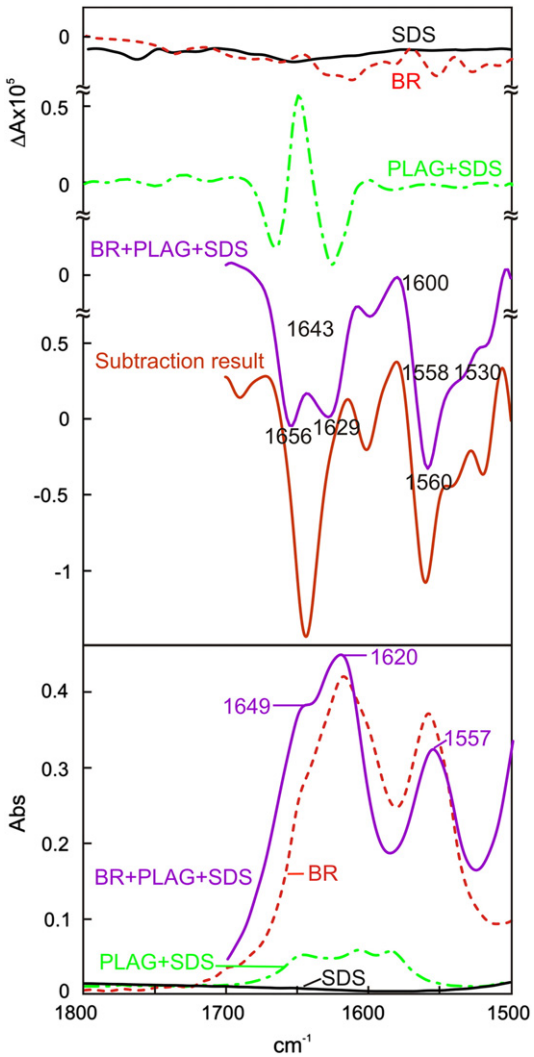

Fig. 8. The VCD (top) and IR (bottom) spectra of SDS micelles, BR (dashed line), PLAG with SDS micelles (dot-and-dash line), BR with PLAG and SDS micelles solution, the difference spectrum of BR with PLAG and SDS micelles solution minus PLAG with SDS micelles solution. ($c_{BR} = 7 \times 10^{-2}$ M, $c_{PLAG} = 4.2 \times 10^{-2}$ M, $c_{SDS} = 5.6 \times 10^{-1}$ M).

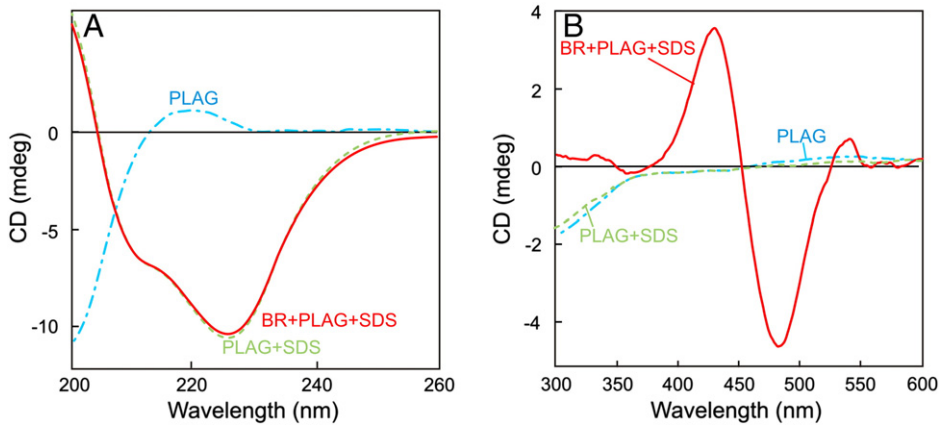

Fig. 9. A, B. The ECD spectra of PLAG (dot-and-dash line), PLAG with SDS micelles (dashed line) and BR with PLAG and SDS micelles (solid line) in the spectral regions typical of PLAG (A) and BR (B). ($c_{BR} = 1 \times 10^{-5}$ M, $c_{PLAG} = 6.4 \times 10^{-4}$ M, $c_{SDS} = 1.1 \times 10^{-2}$ M).

protein, BR preferred to bind to this polypeptide and not to the membrane. Although we had deliberately chosen liposomes and micelles to which BR is not inclined to bind, the VCD clearly showed that the structure of the whole system including the model membranes was still influenced by the presence of BR and by its interaction with the helical polypeptide.

Several tests were also performed with other positively charged polypeptide, poly-L-lysine, bound to the SDS micelles in the β-sheet conformation [36] (results not shown). No interaction of BR was observed in this case, which indicated the importance of the *α-helical* conformation but other tests with different β-sheet peptides are needed.

The observed spectral patterns were not the same for BR in the PLAG/DMPG and PLAG/SDS systems, although PLAG is converted into the *α-helical* conformation in both the systems. Other studies suggest that the size of the head groups of the lipids or surfactants, which formed model membranes, may have a significant impact [60]. The SDS head group is smaller than that of DMPG, so it is possible that the arginine residues are closer when bound to the micelles surface and this influenced the interaction with BR. It probably allowed one form of BR (the M-form) to bind preferentially, while the more opened PLAG/DMPG with a bigger DMPG head group allowed a diversity of BR structures to bind.

4. Conclusions

In this study, the VCD spectroscopy was used for the first time to study the BR interaction with model membranes and models for membrane proteins. We observed the enantioselective interaction of BR with zwitterionic DMPC and SPM liposomes. No interaction of this kind was observed for negative DMPG liposomes. The VCD spectra indicated that BR bound to the DMPC liposomes in the M-form and led to a spatial restriction of lipids accompanied by an enhanced VCD signal. This was also observed for the SPM liposomes which were significantly affected by the presence of BR. The fluorescence emission spectra showed the BR interaction with less polar parts of the DMPC bilayer while the spectra for BR/SPM liposomes system were red shifted documenting the interaction in more polar region.

The strong VCD signal which was induced in the BR/SPM system documented the stability and robustness of the BR/SPM associates and provided explanations for the BR neurotoxicity. The effect of time and pH on the BR/DMPC or SPM liposomes system was shown to be essential while the effect of temperature in the range of 15–70 °C was negligible suggesting the high temperature stability of BR bound to membranes.

A possibility of BR binding to a membrane in the presence of a membrane protein was tested on a model composed of the DMPG liposomes or SDS micelles with PLAG bound to its surface. BR clearly interacted with PLAG, even though its conformation was not easily assigned. In a system with SDS micelles, BR was preferentially bound in the M-form.

These results suggest that BR may endanger the structure of the cell membranes especially at locally increased concentrations. The structure of the SPM liposomes (a simple model for nerve cells) was influenced gravely as a strong, induced VCD signal was observed. In addition, the defense of the human organism might not be sufficient as a mild temperature elevation did not help to prevent BR from an interaction with the model membranes. However, in the presence of α-helical peptide PLAG, BR might incline to bind to the peptide and not to the membrane. Generalization to the effect of α-helical peptides needs further testing with biologically relevant proteins.

Acknowledgement

Financial support from the Specific University Research No. 20/2012 (A2_FCHI_2012_027) and by the Czech Science Foundation (P206/11/0836, P208/11/0105) is gratefully acknowledged.

Appendix A. Supplementary data

Supplementary data to this article can be found online at http://dx.doi.org/10.1016/j.bbamem.2013.12.005.

References

[1] L. Vitek, J.D. Ostrow, Bilirubin chemistry and metabolism; harmful and protective aspects, Curr. Pharm. Des. 15 (2009) 2869–2883.
[2] L. Vítek, Bilirubin a interní choroby: význam pro kliniku a praxi, first ed. Grada Publishing, Praha, 2009.
[3] L. Vitek, L. Sedlackova, P. Branny, T. Ruml, Metabolism of bilirubin and methods of elimination of its toxicity, Chem. Listy 97 (2002) 24–28.
[4] D. Voet, J.G. Voet, Biochemistry, Wiley, New York, 2004, p. 1056.
[5] M.A. Brito, R. Silva, C. Tiribelli, D. Brites, Assessment of bilirubin toxicity to erythrocytes. Implication in neonatal jaundice management, Eur. J. Clin. Investig. 30 (2000) 239–247.
[6] C. Bernardini, P. D'Arrigo, G. Elemento, G. Mancini, S. Servi, A. Sorrenti, The posssible role of enantiodiscrimination in bilirubin toxicity, Chirality 21 (2009) 87–91.
[7] M.A. Brito, C.D. Brondino, J.J.G. Moura, D. Brites, Effects of bilirubin molecular species on membrane dynamic properties of human erythrocyte membranes: a spin label electron paramagnetic resonance spectroscopy study, Arch. Biochem. Biophys. 387 (2001) 57–65.
[8] S.E. Boiadjiev, R.V. Person, D.A. Lightner, Synthesis, intramolecular hydrogen-bonding and conformation of optically-active bilirubin amides—analysis by circular-dichroism and NMR, Tetrahedron-Asymmetry 4 (1993) 491–510.
[9] S.E. Boiadjiev, D.A. Lightner, Exciton chirality of bilirubin homologs, Chirality 9 (1997) 604–615.
[10] S.E. Boiadjiev, D.A. Lightner, Optical activity and stereochemistry of linear oligopyrroles and bile pigments, Tetrahedron-Asymmetry 10 (1999) 607–655.
[11] S.E. Boiadjiev, R.V. Person, G. Puzicha, C. Knobler, E. Maverick, K.N. Trueblood, D.A. Lightner, Absolute-configuration of bilirubin conformational enantiomers, J. Am. Chem. Soc. 114 (1992) 10123–10133.

[12] D. Lightner, R. Person, B. Peterson, G. Puzicha, Y.M. Pu, S. Bojadziev, Conformational-analysis and circular-dichroism of bilirubin, the yellow pigment of jaundice, Biomol. Spectrosc. 1432 (1991) 2–13.
[13] D.A. Lightner, J.K. Gawronski, W.M.D. Wijekoon, Complementarity and chiral recognition—enantioselective complexation of bilirubin, J. Am. Chem. Soc. 109 (1987) 6354–6362.
[14] R.V. Person, B.R. Petersen, D.A. Lightner, Computed exciton coupling circular-dichroism spectra for conformational-analysis of bilirubin, Abstr. Pap. Am. Chem. Soc. 203 (1992) 32(Comp).
[15] A. Sorrenti, B. Altieri, F. Ceccacci, P. Profio, R. Germani, L. Giansanti, G. Savelli, G. Mancini, Deracemization of bilirubin as the marker of the chirality of micellar aggregates, Chirality 24 (2012) 78–85.
[16] M.A. Brito, D. Brites, D.A. Butterfield, A link between hyperbilirubinemia, oxidative stress and injury to neocortical synaptosomes, Brain Res. 1026 (2004) 33–43.
[17] D. Brites, The evolving landscape of neurotoxicity by unconjugated bilirubin: role of glial cells and inflammation, Front. Pharmacol. 3 (2012) 88.
[18] M.J. Daood, A.F. McDonagh, J.F. Watchko, Calculated free bilirubin levels and neurotoxicity, J. Perinatol. 29 (2009) S14–S19.
[19] J.D. Ostrow, L. Pascolo, D. Brites, C. Tiribelli, Molecular basis of bilirubin-induced neurotoxicity, Trends Mol. Med. 10 (2004) 65–70.
[20] L. Rigato, J.D. Ostrow, C. Tiribelli, Bilirubin and the risk of common non-hepatic diseases, Trends Mol. Med. 11 (2005) 277–283.
[21] D.K. Stevenson, H.J. Vreman, R.J. Wong, Bilirubin production and the risk of bilirubin neurotoxicity, Semin. Perinatol. 35 (2011) 121–126.
[22] B.J. Yang, M.D. Morris, M.Q. Xie, D.A. Lightner, Resonance raman-spectroscopy of bilirubins—band assignments and application to bilirubin lipid complexation, Biochemistry 30 (1991) 688–694.
[23] A.K. Masood, S.M. Faisal, M.K. Mushahid, A. Nadeem, M.U. Siddiqui, M. Owais, Binding of bilirubin with albumin-coupled liposomes: implications in the treatment of jaundice, Biochim. Biophys. Acta Biomembr. 1564 (2002) 219–226.
[24] S. Borocci, F. Ceccacci, O. Cruciani, G. Mancini, A. Sorrenti, Chiral recognition in biomembrane models: what is behind a 'simple model', Synlett (2009) 1023–1033.
[25] D. Zakim, P.T.T. Wong, A high-pressure, infrared spectroscopic study of the solvation of bilirubin in lipid bilayers, Biochemistry 29 (1990) 2003–2007.
[26] V. Glushko, M. Thaler, M. Ros, The fluorescence of bilirubin upon interaction with human-erythrocyte ghosts, Biochim. Biophys. Acta 719 (1982) 65–73.
[27] V.Y. Plavskii, V.A. Mostovnikov, G.R. Mostovnikova, A.I. Tret'yakova, Spectral fluorescence and polarization characteristics of Z, Z-bilirubin IXα, J. Appl. Spectrosc. 74 (2007) 120–132.
[28] S.D. Zucker, W. Goessling, J.L. Gollan, Kinetics of bilirubin transfer between serum albumin and membrane vesicles, J. Biol. Chem. 270 (1995) 1074–1081.
[29] S.D. Zucker, W. Goessling, M.L. Zeidel, J.L. Gollan, Membrane lipid composition and vesicle size modulate bilirubin intermembrane transfer, J. Biol. Chem. 269 (1994) 19262–19270.
[30] S.D. Zucker, W. Goessling, E.J. Bootle, C. Sterritt, Localization of bilirubin in phospholipid bilayers by parallax analysis of fluorescence quenching, J. Lipid Res. 42 (2001) 1377–1388.
[31] S.D. Zucker, W. Goessling, A.G. Hoppin, Unconjugated bilirubin exhibits spontaneous diffusion through model lipid bilayers and native hepatocyte membranes, J. Biol. Chem. 274 (1999) 10852–10862.
[32] S.D. Zucker, J. Storch, M.L. Zeidel, J.L. Gollan, Mechanism of the spontaneous transfer of unconjugated bilirubin between small unilamellar phosphatidylcholine vesicles, Biochemistry 31 (1992) 3184–3192.
[33] I. Goncharova, M. Urbanova, Bile pigment complexes with cyclodextrins: electronic and vibrational circular dichroism study, Tetrahedron-Asymmetry 18 (2007) 2061–2068.
[34] I. Goncharova, M. Urbanova, Stereoselective bile pigment binding to polypeptides and albumins: a circular dichroism study, Anal. Bioanal. Chem. 392 (2008) 1355–1365.
[35] I. Goncharova, M. Urbanova, Vibrational and electronic circular dichroism study of bile pigments: complexes of bilirubin and biliverdin with metals, Anal. Biochem. 392 (2009) 28–36.
[36] P. Novotna, M. Urbanova, Vibrational circular dichroism study of polypeptide model-membrane systems, Anal. Biochem. 427 (2012) 211–218.
[37] V. Torchilin, V. Weissig, in: V. Torchilin, V. Weissig (Eds.), Liposomes, Oxford University Press, New York, 2003, pp. 3–8.
[38] A.L. Russell, A.M. Kennedy, A.M. Spuches, D. Venugopal, J.B. Bhonsle, R.P. Hicks, Spectroscopic and thermodynamic evidence for antimicrobial peptide membrane selectivity, Chem. Phys. Lipids 163 (2010) 488–497.
[39] S.Y. Wen, M. Majerowicz, A. Waring, F. Bringezu, Dicynthaurin (ala) monomer interaction with phospholipid bilayers studied by fluorescence leakage and isothermal titration calorimetry, J. Phys. Chem. B 111 (2007) 6280–6287.
[40] T. Wieprecht, O. Apostolov, M. Beyermann, J. Seelig, Membrane binding and pore formation of the antibacterial peptide PGLa: thermodynamic and mechanistic aspects, Biochemistry 39 (2000) 442–452.
[41] T. Wieprecht, O. Apostolov, J. Seelig, Binding of the antibacterial peptide magainin 2 amide to small and large unilamellar vesicles, Biophys. Chem. 85 (2000) 187–198.
[42] T. Wieprecht, M. Beyermann, J. Seelig, Thermodynamics of the coil-alpha-helix transition of amphipathic peptides in a membrane environment: the role of vesicle curvature, Biophys. Chem. 96 (2002) 191–201.
[43] M. Urbanová, P. Maloň, Circular dichroism spectroscopy, in: C. Schalley (Ed.), Analytical Methods in Supramolecular Chemistry, Wiley-VCH, Weinheim, 2012, pp. 337–369.
[44] L.A. Nafie, in: L.A. Nafie (Ed.), Vibrational Optical Activity: Principles and Applications, Wiley, New York, 2011, pp. 237–238.
[45] G. Socrates, Infrared and Raman Characteristic Group Frequencies: Tables and Charts, Wiley-VCH, Chichester, 2001.
[46] B.J. Yang, R.C. Taylor, M.D. Morris, X.Z. Wang, J.G. Wu, B.Z. Yu, G.X. Xu, R.D. Soloway, Normal-coordinate analysis of bilirubin vibrational-spectra—effects of intramolecular hydrogen-bonding, Spectrochim. Acta A 49 (1993) 1735–1749.
[47] R.V. Person, B.R. Peterson, D.A. Lightner, Bilirubin conformational-analysis and circular-dichroism, J. Am. Chem. Soc. 116 (1994) 42–59.
[48] I. Goncharova, S. Orlov, M. Urbanova, Chiroptical properties of bilirubin-serum albumin binding sites, Chirality 25 (2013) 257–263.
[49] P. Mukerjee, J.D. Ostrow, Review: bilirubin pKa studies; new models and theories indicate high pKa values in water, dimethylformamide and DMSO, BMC Biochem. 11 (2010).
[50] J.R. Lakowicz, Principles of Fluorescence Spectroscopy, Springer, Berlin Heidelberg, 2007.
[51] S.E. Boiadjiev, K. Watters, S. Wolf, B.N. Lai, W.H. Welch, A.F. McDonagh, D.A. Lightner, pK(a) and aggregation of bilirubin: Titrimetric and ultracentrifugation studies on water-soluble pegylated conjugates of bilirubin and fatty acids, Biochemistry 43 (2004) 15617–15632.
[52] R. Borstnar, A.R. Choudhury, J. Stare, M. Novic, J. Mavri, Calculation of pK(a) values of carboxylic acids: application to bilirubin, J. Mol. Struct. Thoechem 947 (2010) 76–82.
[53] D.A. Lightner, D.L. Holmes, A.F. McDonagh, On the acid dissociation constants of bilirubin and biliverdin—pK(alpha) values from C-13 NMR spectroscopy, J. Biol. Chem. 271 (1996) 2397–2405.
[54] F.R. Trull, S. Boiadjiev, D.A. Lightner, A.F. McDonagh, Aqueous dissociation constants of bile pigments and sparingly soluble carboxylic acids by C-13 NMR in aqueous dimethyl sulfoxide: Effects of hydrogen bonding, J. Lipid Res. 38 (1997) 1178–1188.
[55] M. Reuter, C. Schwieger, A. Meister, G. Karlsson, A. Blume, Poly-l-lysines and poly-l-arginines induce leakage of negatively charged phospholipid vesicles and translocate through the lipid bilayer upon electrostatic binding to the membrane, Biophys. Chem. 144 (2009) 27–37.
[56] N. Sreerama, R.W. Woody, Circular dichroism of peptides and proteins, in: N. Berova, K. Nakanishi, R.W. Woody (Eds.), Circular Dichroism: Principles and Applications, second ed., Wiley-VCH, New York, 2000, pp. 601–620.
[57] X.M. Cai, C. Dass, Conformational analysis of proteins and peptides, Curr. Org. Chem. 7 (2003) 1841–1854.
[58] R.K. Dukor, T.A. Keiderling, Reassessment of the random coil conformation—vibrational CD study of proline oligopeptides and related polypeptides, Biopolymers 31 (1991) 1747–1761.
[59] R.K. Dukor, T.A. Keiderling, Mutarotation studies of poly-L-proline using FTIR, electronic and vibrational circular dichroism, Biospectroscopy 2 (1996) 83–100.
[60] W.Y. Zhu, T.A. Keiderling, Interaction of reduced lysozyme with surfactants disulfide effects on reformed structure in micelles, Biochim. Biophys. Acta, Proteins Proteomics 1834 (2013) 593–600.